iScience, Volume *24*

Supplemental information

Adipose-mesenchymal stromal cells suppress experimental Sjögren syndrome by IL-33-driven expansion of ST2^{+} regulatory T cells

Ousheng Liu, Junji Xu, Fu Wang, Wenwen Jin, Peter Zanvit, Dandan Wang, Nathan Goldberg, Alexander Cain, Nancy Guo, Yichen Han, Andrew Bynum, Guowu Ma, Songlin Wang, Zhangui Tang, and Wanjun Chen

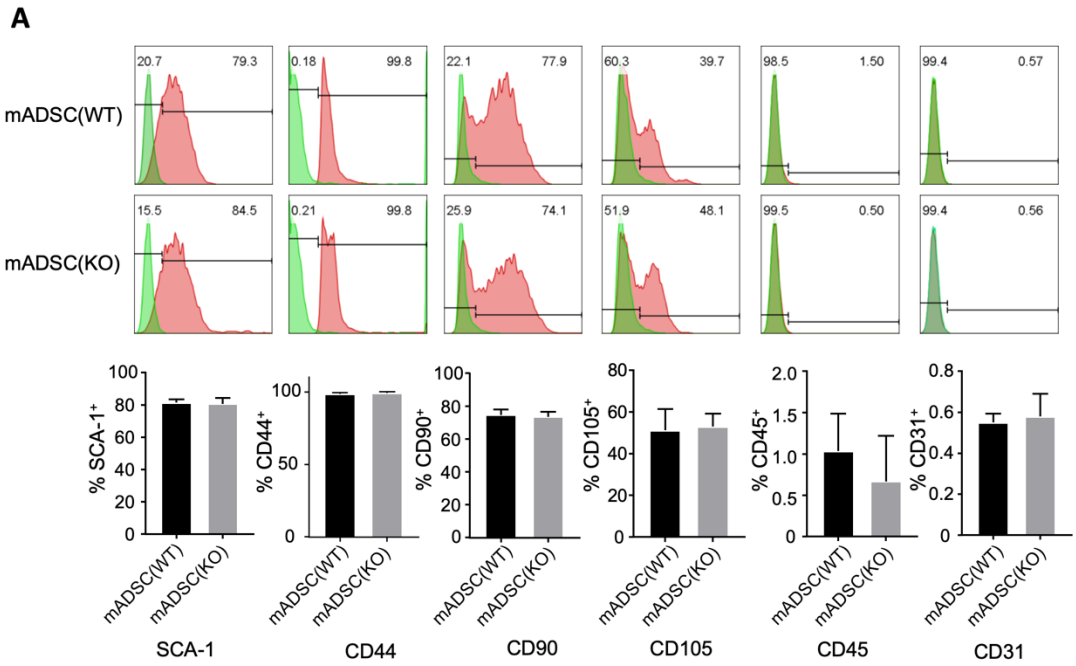
A
mADSC(WT)
mADSC(KO)
20.7
79.3
0.18
99.8
22.1
77.9
60.3
39.7
98.5
1.50
99.4
0.57
15.5
84.5
0.21
99.8
25.9
74.1
51.9
48.1
99.5
0.50
99.4
0.56
% SCA-1+
% CD44+
% CD90+
% CD105+
% CD45+
% CD31+
mADSC(WT)
mADSC(KO)
SCA-1
CD44
CD90
CD105
CD45
CD31

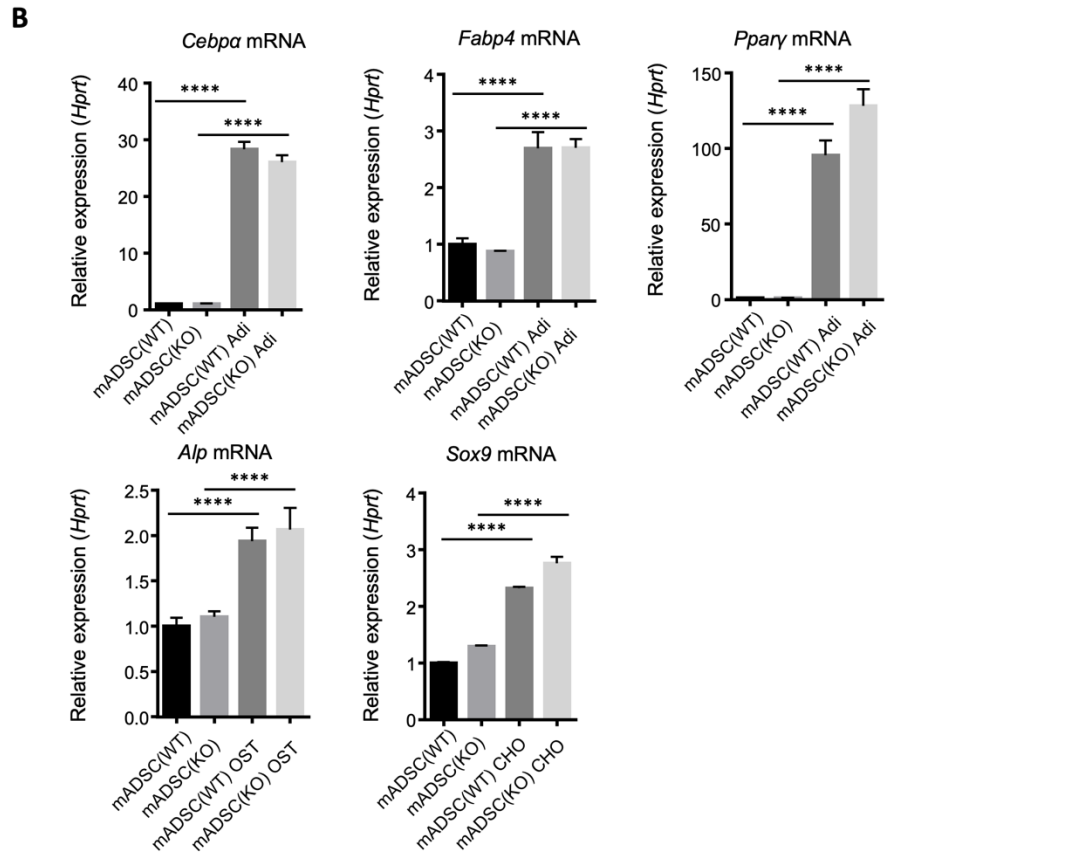
B
Cebpα mRNA
Fabp4 mRNA
Pparγ mRNA
Alp mRNA
Sox9 mRNA
Relative expression (Hprt)
****
mADSC(WT)
mADSC(KO)
mADSC(WT) Adi
mADSC(KO) Adi
mADSC(WT) OST
mADSC(KO) OST
mADSC(WT) CHO
mADSC(KO) CHO

Figure S1. Characterization of the immunophenotype and differentiation potential of mADSC from C57BL/6 or C57BL/6J-*Il33*$^{tm1b(EUCOMM)Cln}$ *in vitro*. Related to Figure 1.

(A) mADSCs from C57BL/6 or C57BL/6J-*Il33*$^{tm1b(EUCOMM)Cln}$ express MSC markers.

(B) mADSCs from C57BL/6 or C57BL/6J-*Il33*$^{tm1b(EUCOMM)Cln}$ were capable of differentiating into adipocytes, osteoblasts, and chondroblast under inductive culture conditions.

Data are pooled from three (A,B) independent experiments. One-way ANOVA was used. Bars, mean; error bars, SEM; ****$P < 0.0001$.

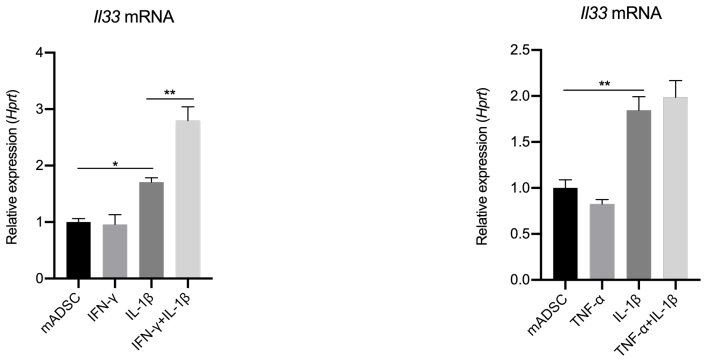

Figure S2. Expression pattern of IL-33 induced by IL-1β synergistically work with TNF-α and IFN-γ. Related Figure 2.

Il33 mRNA expression in mADSC stimulated with indicated combinations of recombinant cytokines (10 ng/ml each) for 6 hr.

Data are pooled from three independent experiments. One-way ANOVA was used. Bars, mean; error bars, SEM; **P*< 0.05, ***P* < 0.01.

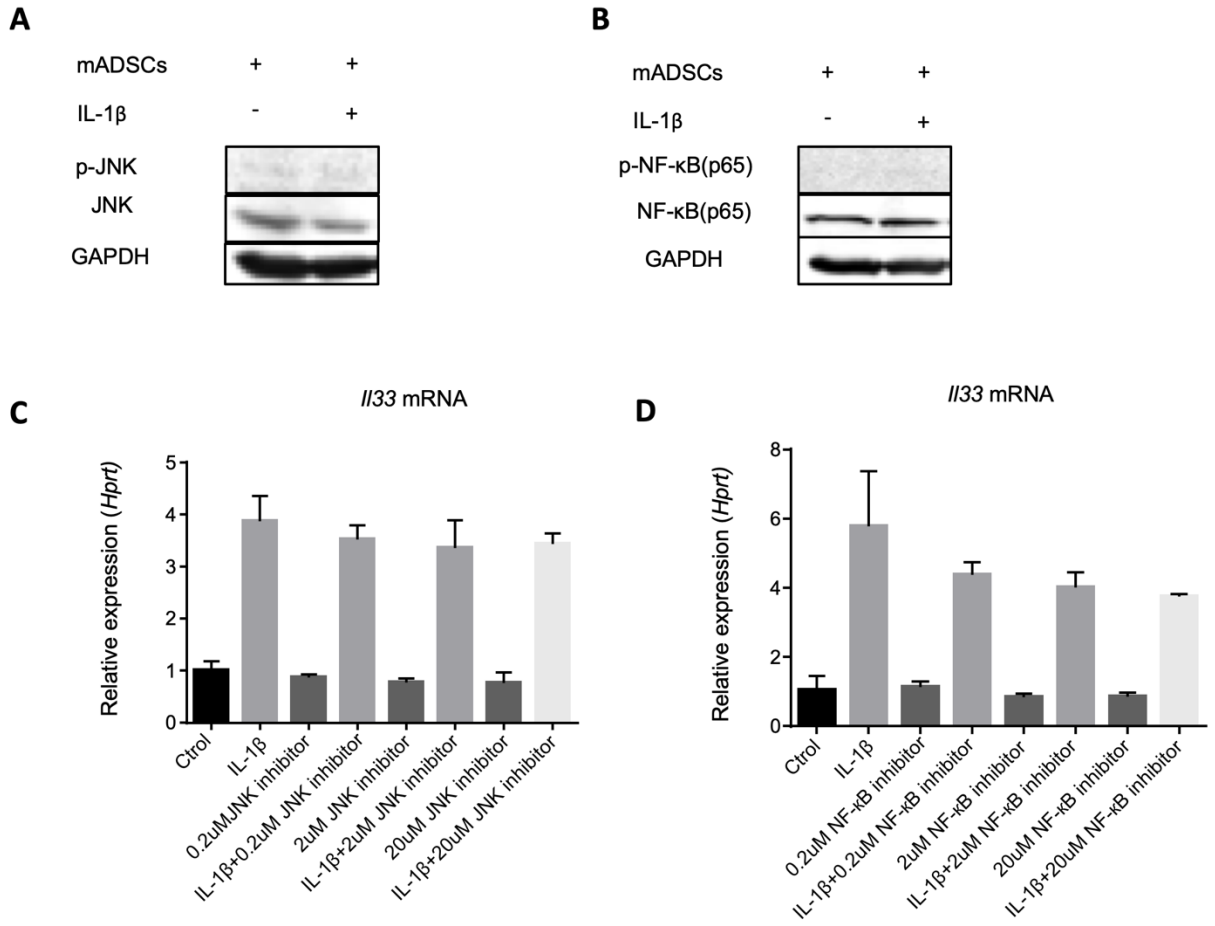

Figure S3. IL-1β upregulates IL-33 expression in mADSC independent on JNK and NF-κB(p65) pathways. Related to Figure 2.

(A) Western blot of p-JNK, JNK, and GAPDH in m ADSC stimulated with or without 2ng/ml IL-1β for 2 hr.

(B) Western blot of p-NF-kB(p65), NF-kB(p65) and GAPDH in m ADSC stimulated with or without IL-1β for 2 hr.

(C) *Il33* mRNA expression in mADSC stimulated for 6 hr with or without 2ng/ml IL-1β plus indicated the concentration of SP600125.

(D) *Il33* mRNA expression in mADSC stimulated for 6 hr with or without 2ng/ml IL-1β plus indicated the concentration of JSH23.

Data are pooled from three (C and D) independent experiments or are representative of three (A and B) independent experiments. In (C and D), one-way ANOVA was used. Bars, mean; error bars, SEM.

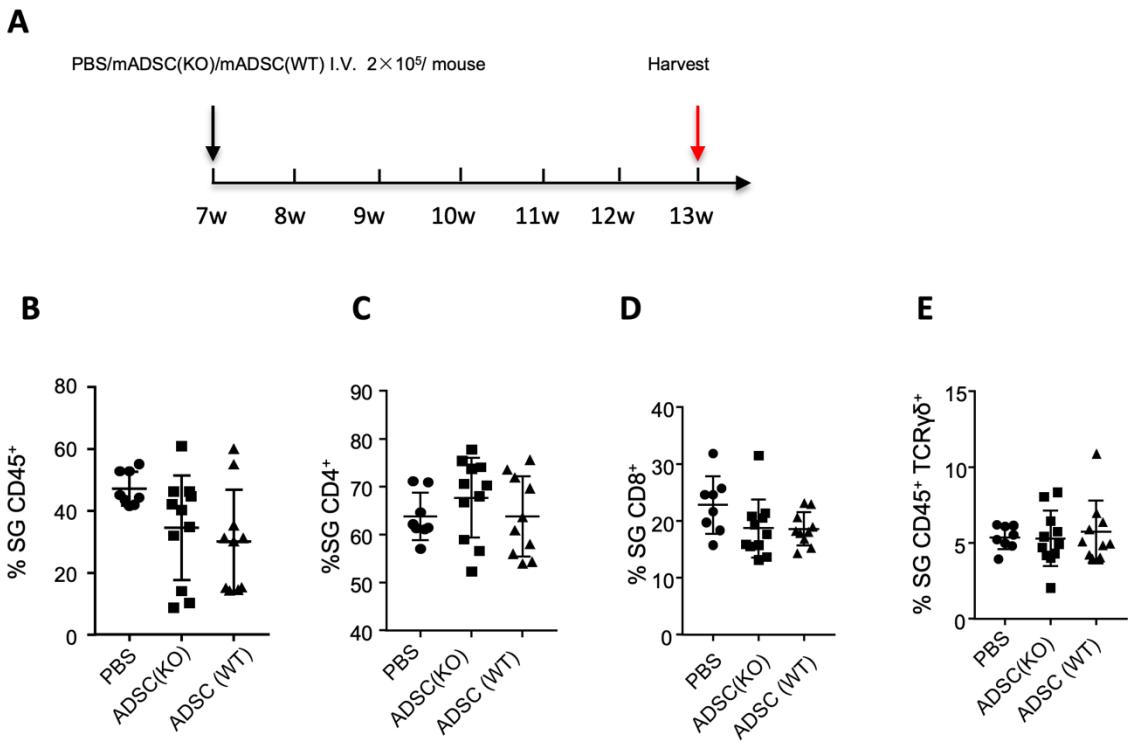

Figure S4. CD45⁺ immune cells express in the submandibular glands of NOD/Ltj mice injected with PBS, ADSC from WT or *Il33*$^{-/-}$ mice. Related to Figure 4.

(A) Experimental workflow of allogeneic mADSCs from WT or il33$^{-/-}$ mice, or PBS infused to NOD/Ltj mice at 7 weeks of age.

(B) Frequency of CD45⁺ cells in the submandibular glands of NOD/Ltj mice injected with PBS, ADSC from WT or *Il33*$^{-/-}$ mice.

(C) Frequency of CD45⁺TCRβ⁺CD4⁺ cells in the submandibular glands of NOD/Ltj mice injected with PBS, ADSC from WT or *Il33*$^{-/-}$ mice.

(D) Frequency of CD45⁺ TCRβ⁺CD8⁺ cells in the submandibular glands of NOD/Ltj mice injected with PBS, ADSC from WT or *Il33*$^{-/-}$ mice.

(E) Frequency of CD45⁺ TCRγδ⁺ cells in the submandibular glands of NOD/Ltj mice injected with PBS, ADSC from WT or *Il33*$^{-/-}$ mice. Data are pooled from three independent experiments. One-way ANOVA was used. Bars, mean; error bars, SEM.

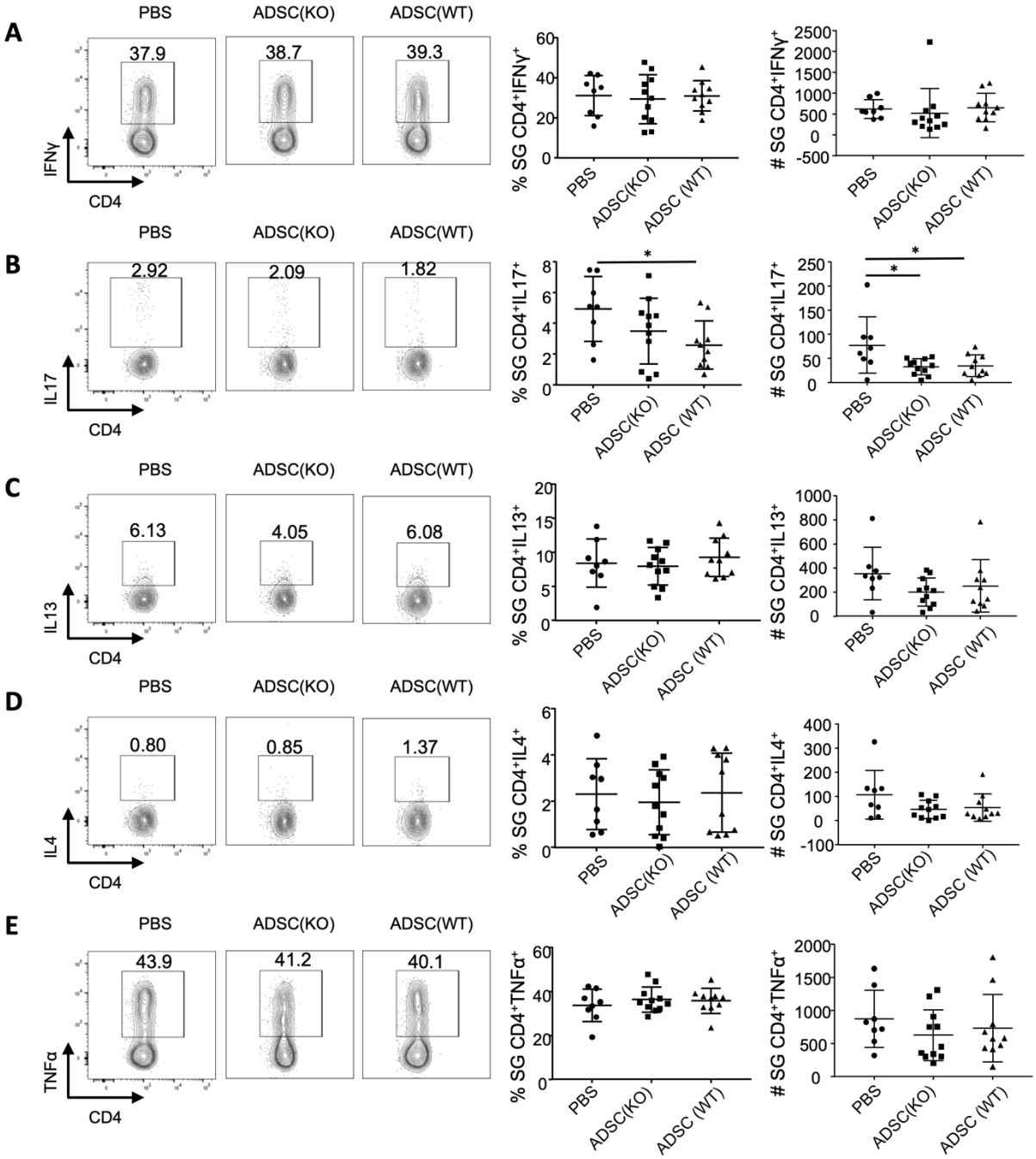
A
PBS
ADSC(KO)
ADSC(WT)
37.9
38.7
39.3
IFNγ
CD4
% SG CD4+IFNγ+
# SG CD4+IFNγ+
B
2.92
2.09
1.82
IL17
CD4
% SG CD4+IL17+
# SG CD4+IL17+
C
6.13
4.05
6.08
IL13
CD4
% SG CD4+IL13+
# SG CD4+IL13+
D
0.80
0.85
1.37
IL4
CD4
% SG CD4+IL4+
# SG CD4+IL4+
E
43.9
41.2
40.1
TNFα
CD4
% SG CD4+TNFα+
# SG CD4+TNFα+

Figure S5. Cytokine expression in TCRβ$^+$CD4$^+$ cells in the submandibular glands of NOD/Ltj mice injected with ADSCs from WT or *Il33*$^{-/-}$ mice. Related to Figure 5.

(A) Frequency and absolute numbers of IFNγ$^+$ in TCRβ$^+$CD4$^+$ cells in the submandibular glands of NOD/Ltj mice injected with PBS, ADSC from WT or *Il33*$^{-/-}$ mice.

(B) Frequency and absolute numbers of IL-17$^+$ in TCRβ$^+$CD4$^+$ cells in the submandibular glands of NOD/Ltj mice injected with PBS, ADSC from WT or *Il33*$^{-/-}$ mice.

(C) Frequency and absolute numbers of IL-13$^+$ in TCRβ$^+$CD4$^+$ cells in the submandibular glands of NOD/Ltj mice injected with PBS, ADSC from WT or *Il33*$^{-/-}$ mice.

(D) Frequency and absolute numbers of IL-4$^+$ in TCRβ$^+$CD4$^+$ cells in the submandibular glands of NOD/Ltj mice injected with PBS, ADSC from WT or *Il33*$^{-/-}$ mice.

(E) Frequency and absolute numbers of TNF-α$^+$ in TCRβ$^+$CD4$^+$ cells in the submandibular glands of NOD/Ltj mice injected with PBS, ADSC from WT or *Il33*$^{-/-}$ mice.

Data are pooled from three independent experiments. One-way ANOVA was used. Bars, mean; error bars, SEM; *P< 0.05.

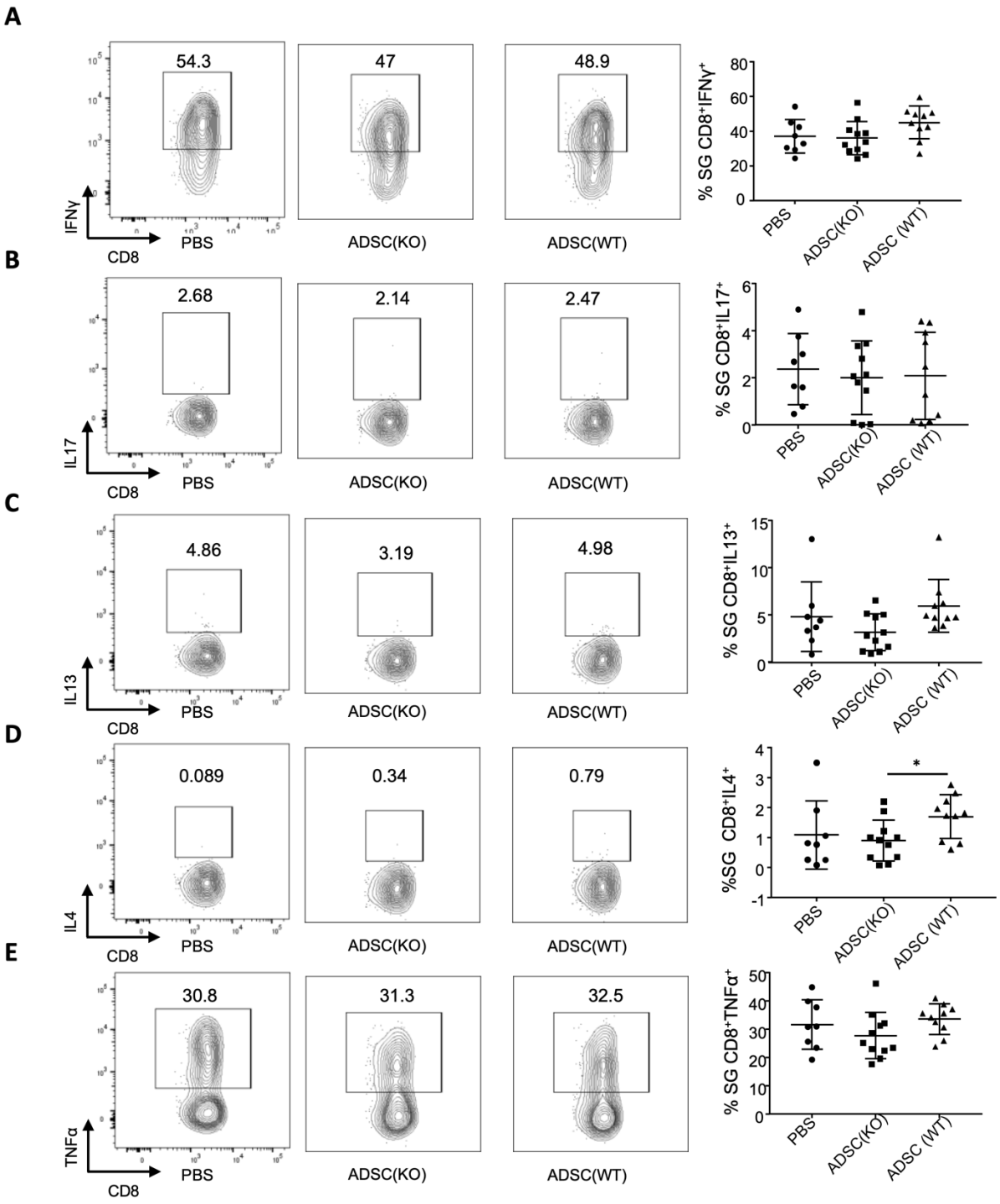
A
54.3
47
48.9
IFNγ
CD8
PBS
ADSC(KO)
ADSC(WT)
% SG CD8+IFNγ+
80
60
40
20
0
PBS
ADSC(KO)
ADSC (WT)
B
2.68
2.14
2.47
IL17
CD8
PBS
ADSC(KO)
ADSC(WT)
% SG CD8+IL17+
6
4
2
0
PBS
ADSC(KO)
ADSC (WT)
C
4.86
3.19
4.98
IL13
CD8
PBS
ADSC(KO)
ADSC(WT)
% SG CD8+IL13+
15
10
5
0
PBS
ADSC(KO)
ADSC (WT)
D
0.089
0.34
0.79
IL4
CD8
PBS
ADSC(KO)
ADSC(WT)
%SG CD8+IL4+
*
4
3
2
1
0
-1
PBS
ADSC(KO)
ADSC (WT)
E
30.8
31.3
32.5
TNFα
CD8
PBS
ADSC(KO)
ADSC(WT)
% SG CD8+TNFα+
50
40
30
20
10
0
PBS
ADSC(KO)
ADSC (WT)

Figure S6. Cytokine expression in TCRβ$^+$CD8$^+$ cells in the submandibular glands of NOD/Ltj mice treated with ADSCs from WT or *Il33*$^{-/-}$ mice. Related to Figure 5.

(A) Frequency of IFNγ$^+$ in TCRβ$^+$CD8$^+$ cells in the submandibular glands of NOD/Ltj mice injected with PBS, ADSC from WT or *Il33*$^{-/-}$ mice.

(B) Frequency of IL17$^+$ in TCRβ$^+$CD8$^+$ cells in the submandibular glands of NOD/Ltj mice injected with PBS, ADSC from WT or *Il33*$^{-/-}$ mice.

(C) Frequency of IL13$^+$ in TCRβ$^+$CD8$^+$ cells in the submandibular glands of NOD/Ltj mice injected with PBS, ADSC from WT or *Il33*$^{-/-}$ mice.

(D) Frequency of IL4$^+$ in TCRβ$^+$CD8$^+$ cells in the submandibular glands of NOD/Ltj mice injected with PBS, ADSC from WT or *Il33*$^{-/-}$ mice.

(E) Frequency TNFα$^+$ in TCRβ$^+$CD8$^+$ cells in the submandibular glands of NOD/Ltj mice injected with PBS, ADSC from WT or *Il33*$^{-/-}$ mice.

Data are pooled from three independent experiments. One-way ANOVA was used. Bars, mean; error bars, SEM; *P< 0.05.

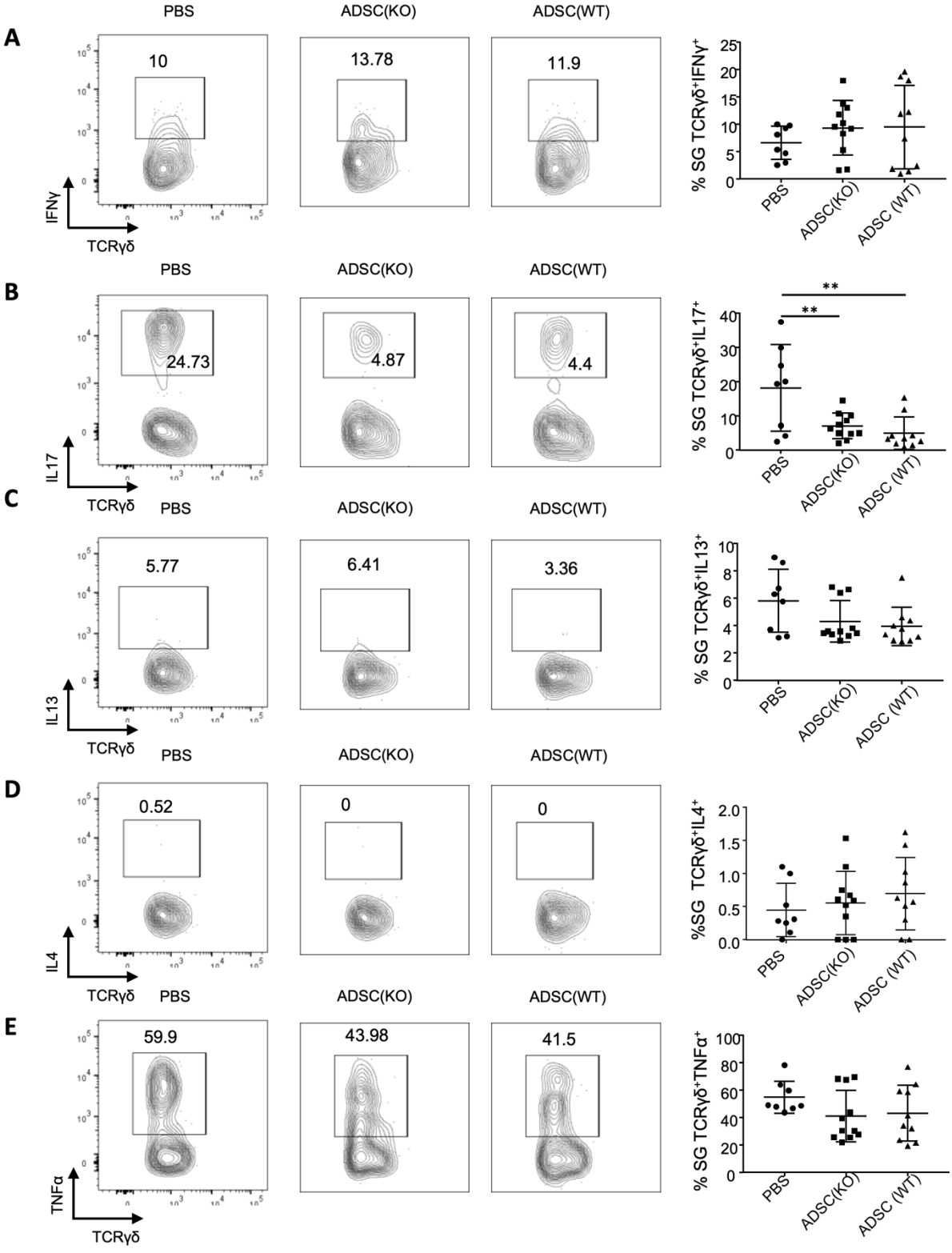
A
PBS
ADSC(KO)
ADSC(WT)
10
13.78
11.9
IFNγ
TCRγδ
% SG TCRγδ+IFNγ+
PBS
ADSC(KO)
ADSC (WT)
B
PBS
ADSC(KO)
ADSC(WT)
24.73
4.87
4.4
IL17
TCRγδ
**
**
% SG TCRγδ+IL17+
PBS
ADSC(KO)
ADSC (WT)
C
PBS
ADSC(KO)
ADSC(WT)
5.77
6.41
3.36
IL13
TCRγδ
% SG TCRγδ+IL13+
PBS
ADSC(KO)
ADSC (WT)
D
PBS
ADSC(KO)
ADSC(WT)
0.52
0
0
IL4
TCRγδ
%SG TCRγδ+IL4+
PBS
ADSC(KO)
ADSC (WT)
E
PBS
ADSC(KO)
ADSC(WT)
59.9
43.98
41.5
TNFα
TCRγδ
% SG TCRγδ+TNFα+
PBS
ADSC(KO)
ADSC (WT)

Figure S7. Cytokine expression in TCRγδ$^+$ cells in the submandibular glands of NOD/Ltj mice treated with ADSCs from WT or *Il33*$^{-/-}$ mice. Related to Figure 5.

(A) Frequency of IFNγ$^+$ in TCRγδ$^+$ cells in the submandibular glands of NOD/Ltj mice injected with PBS, ADSC from WT or *Il33*$^{-/-}$ mice.

(B) Frequency of IL17$^+$ in TCRγδ$^+$ cells in the submandibular glands of NOD/Ltj mice injected with PBS, ADSC from WT or *Il33*$^{-/-}$ mice.

(C) Frequency of IL13$^+$ in TCRγδ$^+$ cells in the submandibular glands of NOD/Ltj mice injected with PBS, ADSC from WT or *Il33*$^{-/-}$ mice.

(D) Frequency of IL4$^+$ in TCRγδ$^+$ cells in the submandibular glands of NOD/Ltj mice injected with PBS, ADSC from WT or *Il33*$^{-/-}$ mice.

(E) Frequency of TNFα$^+$ in TCRγδ$^+$ cells in the submandibular glands of NOD/Ltj mice injected with PBS, ADSC from WT or *Il33*$^{-/-}$ mice. Data are pooled from three independent experiments. One-way ANOVA was used. Bars, mean; error bars, SEM; $^{**}P < 0.01$.

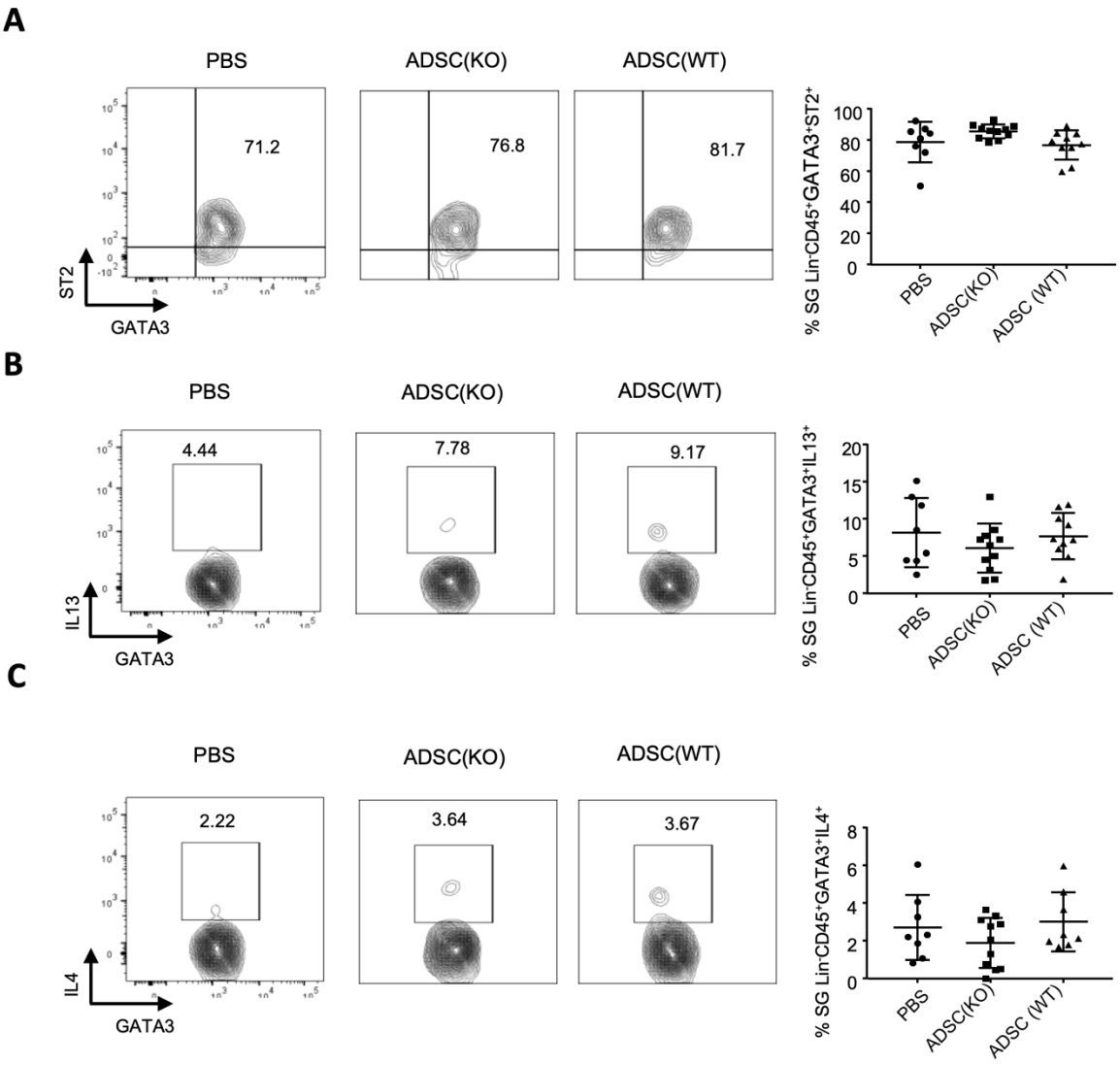

Figure S8. ST2, IL-13, and IL-4 express in ILC2 in the submandibular glands of NOD/Ltj mice injected with ADSCs from WT or *Il33*$^{-/-}$ mice. Related to Figure 5.

(A)The frequency of ST2^{+} in ILC2 in the submandibular glands of NOD/Ltj mice injected with PBS, ADSC from WT or *Il33*$^{-/-}$ mice.

(B) The frequency of IL-13^{+} in ILC2 in the submandibular glands of NOD/Ltj mice injected with PBS, ADSC from WT or *Il33*$^{-/-}$ mice.

(C) The frequency of IL-4^{+} in ILC2 in the submandibular glands of NOD/Ltj mice injected with PBS, ADSC from WT or *Il33*$^{-/-}$ mice.

Data are pooled from three independent experiments. One-way ANOVA was used. Bars, mean; error bars, SEM.

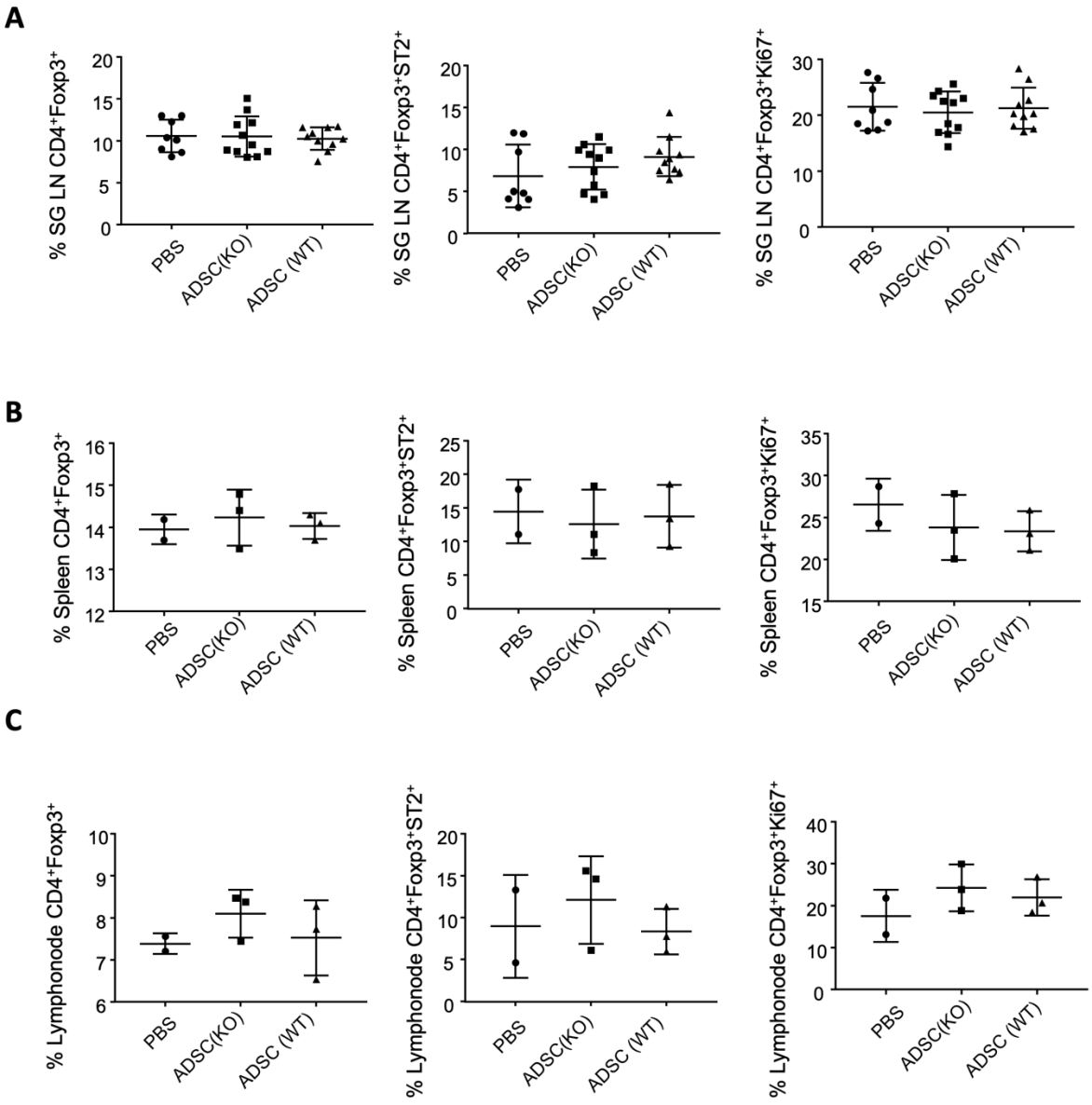

Figure S9. Tregs in the Spleen and lymph nodes of NOD/Ltj mice treated with ADSCs from WT or *Il33*$^{-/-}$ mice. Related to Figure 5.

(A) Frequency of CD4^{+}Foxp3^{+} T, ST2 in Treg and Ki67 in Treg cells in the submandibular lymph node of NOD/Ltj mice injected with PBS, ADSC from WT or *Il33*$^{-/-}$ mice.

(B) Frequency of CD4^{+}Foxp3^{+} T, ST2 in Treg and Ki67 in Treg cells in the spleen of NOD/Ltj mice injected with PBS, ADSC from WT or *Il33*$^{-/-}$ mice.

(C) Frequency of CD4^{+}Foxp3^{+} T, ST2 in Treg and Ki67 in Treg cells in the armpit and inguinal lymph nodes of NOD/Ltj mice injected with PBS, ADSC from WT or *Il33*$^{-/-}$ mice.

Data (A) are pooled from three independent experiments. Data (B and C) are pooled from two independent experiments. One-way ANOVA was used. Bars, mean; error bars, SEM.

Transparent Methods

Mice

Male mice *C57BL/6*, Female NOD/ShiLtj mice *(Cdh23ahl)* mice were purchased from The Jackson Laboratory. Male *mice C57BL/6J- Il33*$^{tm1b(EUCOMM)Cln}$ were donated by Washington University at St. Louis. All animal studies were approved by the Animal Care and Use Committees of National Institute of Dental and Craniofacial Research, National Institutes of Health. 6 to10 weeks old mice were used for all experiments.

Mice/human ADSCs culture

ADSCs were prepared from *C57BL/6* or *C57BL/6J-Il33*$^{tm1b(EUCOMM)Cln}$ subcutaneous fat as described previously[1] and cultured for 2 weeks. Human ADSCs were purchased from Lonza Walkersville Inc, which were isolated from healthy (non-diabetic) adult lipoaspirates collected during elective surgical liposuction procedures. Mice and human ADSCs were cultured in alpha-minimum essential medium containing 20% fetal calf serum and 1% antibiotic-antimycotic (Gibco) in a 5%CO_2 incubator at 37℃. In brief, tissue was minced with two scalpels (crossed blades) and then incubated in a 0.5% collagenase I/phosphate buffered saline (PBS) solution (Collagenase Type: CLS, Biochrom, Berlin, Germany; PBS, Sigma, Taufkirchen, Germany) for 40min at 37°C under constant shaking. The digested tissue solution was then separated through a 100 μm strainer, and the resulting filtrate was centrifuged at 300 g for 5 min. The resulting pellet was washed twice with medium and centrifuged again at 300 g for 5 min. Finally, cells were plated for initial cell culture and cultured at 37°C in an atmosphere of 5% CO_2 in the humid air. alpha-minimum essential medium (α-MEM, Gibco) with a physiologic glucose concentration (100 mg/dL) and used as a standard culture medium. The medium was replaced every three days. Subconfluent cells (90%) were passaged by trypsinization. Cells between passages 2 and 3 were used throughout the experiments. Cell morphology was examined by phase contrast microscopy.

$CD4^+CD25^+$Treg isolation and culture

$CD4^+CD25^+$Tregs from spleen and lymph node from C57BL/6 mice were purified by magnetic cell sorting (Miltenyi Biotec). Tregs were cultured in completed DMEM with or without ADSCs lysates.

ADSCs lysates preparation

ADSCs from WT or *Il33*$^{-/-}$ mice were cultured with IL-1β for 72h. Then ADSCs were broken with ultrasonic method (output power 500W, twice, 5min/each, 4℃) and centrifuged at 14000rpm for 20min.Then the supernatant was collected. $CD4^+CD25^+$Tregs were cultured with IL-1β-stimulated WT or *Il33*$^{-/-}$ ADSC lysates for 24h and 72h with indicated concentration of plate-bound 1μg/ml anti-CD3, 1μg/ml soluble anti-CD28 and 100U/ml IL-2 for 3 days. *Il1rl1* mRNA in Tregs and $ST2^+$Treg were detected by real-time PCR and flow cytometry analysis.

Real-time PCR

Total RNA was derived from cells using RNeasy Mini Kit (QIAGEN) and reversed transcribed using High Capacity cDNA Reverse Transcription Kit (Applied Biosystems). Quantitative real-time PCR was performed according to the protocol of TaqMan Gene Expression Master Mix (Applied Biosystems) with the following TaqMan primers: Hprt, Mm00446968_m1; MmIl33, Mm00505403_m1; MmSt2, Mm00516117_m1; MmCebpα, Mm00514283_s1; MmFabp4, Mm00445878_m1; MmPpar, Mm01184322_m1; MmAlp, Mm00475834_m1; MmSox9, Mm00448840_m1; MmGapdh, Mm99999915_g1; MmFoxp3, Mm00475162_m1; Human Gapdh Hs02758991_m1; Human Il33, Hs04931857_m1.

Western blot analysis

Protein was extracted using RIPA buffer containing proteinase inhibitor cocktail and quantified with a Bio-Rad protein assay. An equal amount of protein was separated on SDS-polyacrylamide gels in a Tris/SDS buffer system and then transferred onto nitrocellulose membranes. Blotting was performed according to standard procedures with primary antibodies against IL-33, ERK, p38, JNK, NF-κB(p65), p-ERK, p-p38, p-JNK, p-NF-κB (p65), β-actin and GAPDH overnight, followed by incubation with appropriate fluorescence-conjugated secondary antibodies. The proteins of interest were analyzed using an Odyssey IR scanner, and signal intensities were quantified using NIH Image/J software.

ELISA assays
To evaluate protein levels of IL-33 in cell lysates and cell culture supernatants, ELISA assays were performed by ELISA kits from R&D Systems according to the manufacturer's instruction.

Flow cytometry analysis
For intracellular cytokine staining, cells were stimulated with PMA (50 ng/ml), Ionomycin (250 ng/ml) and Golgi-Plug (1:1000 dilution, BD PharMingen) at 37℃ for 4h, followed by fixation with the Fixation/Permeabilization buffer solution (BD Biosciences) according to manufacturer's instruction. The staining procedures for MOG38-49-specific tetramer were previously described[2]. Stained cells were analyzed on an LSRFortessa (BD Biosciences), and data were analyzed with FlowJo software.

Allogeneic ADSCs treatment and saliva flow rate measurement
Allogeneic ADSCs from mice *C57BL/6J* or *C57BL/6J-Il33*$^{tm1b(EUCOMM)Cln}$ treatment and saliva flow rate measurement, For ADSCs treatment, NOD/ShiLtj mice were injected with 1*105 ADSCs (from *C57BL/6* or *C57BL/6J-Il33*$^{tm1b(EUCOMM)Cln)}$ in 0.10 ml PBS via the tail vein. Mice were injected with isoproterenol/pilocarpine to stimulate saliva secretion. For saliva flow rate test, mice were weighed, and mild anesthesia was induced with a solution of Ketamine and Xylazine (20 mg/ml; Sigma) in sterile water, given intraperitoneally (1 μl/g of body weight). Salivary secretion was stimulated using 0.1 ml/kg body weight of a pilocarpine solution (50 mg/ml) subcutaneously. Saliva collection began within two minutes of pilocarpine administration. Animals were positioned with a 75-mm hematocrit tube placed in the oral cavity, and the whole saliva was collected into pre-weighed 0.75 ml Eppendorf tubes for 10 minutes. The amount of saliva collected was determined gravimetrically.

Histology
Salivary glands were collected and fixed in 10% formalin (Richard-Allan Scientific), embedded in paraffin, cut longitudinally into 5-mm sections and stained with hematoxylin and eosin. Images were acquired using Aperio digital pathology system and processed in Aperio ImageScope v11.1.2.752 software and the area of inflammatory focus (containing>50 lymphocytes per 4mm^2 tissue) was calculated per field at X200 magnification by Image-Pro Plus Version 6.0 software (Media Cybernetics). Five entire salivary gland sections for each animal were counted with an average of 10 fields by an expert of histopathology under blinded fashion.

Statistics
All data have a normal distribution and are presented as mean ± standard error of the mean (SEM; in data of infiltrating area statistics) or standard deviation (in other data) of three independent experiments, and we used an α level of 0.05 for all statistical tests. The mice salivary flow rates were statistically analyzed with repeated measurement; other data were analyzed with student's t-test, one-way analysis of variance (ANOVA), or two-way ANOVA. All *P* value less than 0.05 were considerate significant. Statistical analysis was done with Graphpad Prism 7.

Regent or Resource source identifier
Antibodies Purified anti-mouse CD3 (145-2C11) Bio X Cell Cat# BE0001-1; RRID: AB_1107634
Purified anti-mouse CD28 (37.51) Bio X Cell Cat# BE0015-1; RRID: AB_1107624
Anti-mouse CD4 Alexa Fluor 405(RM4-5) eBioscience Cat# MCD0426; RRID: AB_1473885
Anti-mouse CD4 Alexa Fluor 700 (RM4-5) eBioscience Cat# 56-0042-82; RRID: AB_494000
Anti-mouse CD4 PerCP-Cy5.5 (RM4-5) eBioscience Cat# 45-0042-82; RRID: AB_1107001
Anti-mouse CD4 PE-Cy7 (RM4-5) eBioscience Cat# 25-0042-82; RRID: AB_469578
Anti-mouse CD8a PerCP-Cy5.5 (53-6.7) eBioscience Cat# 45-0081-82; RRID: AB_1107004
Anti-mouse CD8b FITC (eBioH35-17.2 (H35-17.2)) eBioscience Cat# 11-0083-82; RRID: AB_657764
Anti-mouse CD62L PE (MEL-14) eBioscience Cat# 12-0621-82; RRID: AB_465721
Anti-mouse CD44 APC (IM7) eBioscience Cat# 17-0441-82; RRID: AB_469390
Anti-mouse CD45 Alexa Fluor 700 (30-F11) eBioscience Cat# 56-0451-82; RRID: AB_891454
Anti-mouse CD45 Pacific Blue (30-F11) eBioscience Cat# MCD4528; RRID: AB_1500474
Anti-mouse CD25 PE (PC61.5) eBioscience Cat# 12-0251-82; RRID: AB_465607
Anti-mouse TCRβ APC-Cy7(H57-597) eBioscience Cat# 47-5961-82; RRID: AB_1272173
Anti-mouse TCRγδ Percp-eFlour710 (eBioGL3 (GL-3, GL3)) Cat# 46-5711-82; RRID: AB_2016707

Anti-mouse/rat Foxp3 eFluor 450 (FJK-16a) eBioscience Cat# 48-5773-82; RRID: AB_1518812
Anti-mouse IL-4 PE-Cy7 (11B11) eBioscience Cat# 25-7041-82; RRID: AB_2573520
Anti-mouse IL-10 APC-Cy7 biolegend Cat# 505036; RRID: AB_2566331
Anti-mouse IL-13 PE (eBio13A) eBioscience Cat# 12-7133-82; RRID: AB_763559
Anti-mouse IL-13 PE-eFluor610 (eBio13A) eBioscience Cat# 61-7133-82; RRID: AB_2574654
Anti-mouse IL-17A APC (eBio17B7) eBioscience Cat# 25-7177-82; RRID: AB_10732356
Anti-mouse IFN-γ eFluor 450 (XMG1.2) eBioscience Cat# 48-7311-82; RRID: AB_1834366
Anti-mouse TNF-α PE-ef610 (MP6-XT22) eBioscience Cat# 61-7321-82; RRID: AB_2574666
Anti-mouse-Ki-67 PE-ef610 (SolA15) eBioscience Cat # 61-5698-82; RRID: AB_2574620
Anti-mouse CD3 PerCP-Cyanine5.5 eBioscience Cat # 45-0031-82; RRID: AB_1107000
Anti-mouse Ly-6G/Ly-6C (RB6-8C5), PerCP-Cyanine5.5 eBioscience Cat #45-5931-80; RRID: AB_906247
Anti-mouse CD19 (eBio1D3 (1D3)) PerCP-Cyanine5.5 eBioscience Cat # 45-0193-82; RRID: AB_1106999
Anti-mouse B220 (RA3-6B2) PerCP-Cyanine5.5 eBioscience Cat # 45-0452-82; RRID: AB_1107006
Anti-mouse CD11c (N418) PerCP-Cyanine5.5 eBioscience Cat # 45-0114-82; RRID: AB_925727
Anti-mouse CD11b (M1/70) PerCP-Cyanine5.5 eBioscience Cat # 45-0112-82; RRID: AB_953558
Anti-mouse Fc PerCP-Cyanine5.5 biolegend Cat # 149517; RRID: AB_2632750
Anti-mouse TCRβ (H57-597) PerCP-Cyanine5.5 eBioscience Cat # 45-5961-82; RRID: AB_925763
Anti-mouse NK1.1 (PK136) PerCP-Cyanine5.5 eBioscience Cat # 45-5941-82; RRID: AB_914361
Anti-mouse CD127 (A7R34) Alexa Fluor 700 eBioscience Cat # 56-1271-82; RRID: AB_657611
Anti-mouse Ly-6A/E (Sca-1) (D7) FITC eBioscience Cat # 11-5981-82; RRID: AB_465333
Anti-mouse ST2 (RMST2-2) PE eBioscience Cat # 12-9335-82; RRID: AB_2572708
Anti-mouse ST2 (RMST2-2) Percp-eFluor710 eBioscience Cat # 46-9335-82; RRID: AB_2573883
Anti-mouse GATA3 (RMST2-2) Percp-eFluor710 eBioscience Cat # 46-9335-82; RRID: AB_2573883
Anti-IL-33 antibody [Nessy-1] abcam Cat #ab54385; RRID: AB_881109
P44/42 MAPK(Erk1/2) (L34F12) mouse mAb CST Cat# 4696 ; RRID:AB_390780
Phospho- P44/42 MAPK(Erk1/2) (Thr202/Tyr204) (197G2) Rabbit mAb CST Cat# 4377; RRID:AB_331775
p38 MAPK (D13E1) XP Rabbit mAb CST Cat #8690; RRID:AB_10999090
Phospho-p38 MAPK (Thr180/Tyr182) (28B10) Mouse mAb Cat #9216; RRID:AB_331296
Anti-JNK1+JNK2+JNK3 antibody [EPR16797-211] abcam Cat #ab179461; RRID: AB_2744672
Phospho-SAPK/JNK (Thr183/Tyr185) (81E11) Rabbit mAb Cat #4668; RRID:AB_823588
p65 rabbit mAb (C22B4) CST Cat# 4764; RRID:AB_823578
Phospho-p65 (Ser536) rabbit mAb (93H1) CST Cat# 3033; RRID:AB_331284
GAPDH rabbit mAb (14C10) CST Cat# 2118; RRID:AB_561053

Chemicals, Peptides, and Recombinant Proteins
Recombinant human IL-2 R&D Systems Cat# 202-IL-500
Recombinant human TGF-β1 R&D Systems Cat# 240-B-010
Recombinant mouse IL-1β PeproTech Cat# 211-11B
Recombinant mouse IL-4 PeproTech Cat# 214-14
Recombinant mouse IL-5 PeproTech Cat# 215-15
Recombinant mouse IL-6 PeproTech Cat# 216-16
Recombinant mouse IL-7 PeproTech Cat# 217-17
Recombinant mouse IL-12 PeproTech Cat# 210-12
Recombinant mouse IL-13 PeproTech Cat# 210-13
Recombinant mouse IL-15 PeproTech Cat# 210-15
Recombinant mouse IL-21 R&D Systems Cat# 594-ML-025
Recombinant mouse IL-22 R&D Systems Cat# 582-ML-010
Recombinant mouse IL-23 R&D Systems Cat# 1887-ML-010
Recombinant mouse/rat IL-33 R&D Systems Cat# M3300
Recombinant mouse TNF-α PeproTech Cat# 315-01A
Recombinant mouse IFN-γ PeproTech Cat# 315-05
Recombinant Human IL-1β PeproTech Cat# 200-01B
(5Z)-7-Oxozeaenol R&D Systems Cat# 3604/1
U0126 R&D Systems Cat# 1144/25
SB203580 R&D Systems Cat# 1202/10
SP600125 Invitrogen Cat# tlrl-sp60

JSH23 ab144824 abcam Cat#749886-87-1
PMA Sigma Aldrich Cat# P1585
Ionomycin Sigma Aldrich Cat# I0634
Golgi-Plug BD Biosciences Cat# 555029
TRIzol reagent Invitrogen Cat# 15596026
DNase I Sigma Alcrich Cat# DN25
Collagenase GIBCO Cat# 17104019

Regent or Resource source identifier RNeasy
Mini Kit QIAGEN Cat# 74106
High-Capacity cDNA Reverse Transcription Kit Applied Biosystems Cat# 4368814
TaqMan Gene Expression Master Mix Applied Biosystems Cat# 4369016
Foxp3/Transcription Factor Staining Buffer Set eBioscience Cat# 00-5523-00
Cytofix/Cytoperm Fixation/ Permeabilization Solution Kit BD Biosciences Cat# 554714
$CD4^+$ T cell isolation kit, mouse Miltenyi Biotec Cat # 130-104-456
CD4+CD25+ Regulatory T Cell Isolation Kit, mouse Miltenyi Biotec Cat# 130-091-041

Experimental Models: Cell Lines
hADSC Human Adipose-Derived Stem Cells Catalog #: PT-5006, Lonza Walkersville Inc

Experimental Models: Organisms/Strains
Mouse: C57BL/6 The Jackson Laboratory Cat#000664
Mouse: C57BL/6J-Il33$^{tm1b(EUCOMM)Cln}$ Washington university at St. Louis
Mouse: NOD/ShiLtj The Jackson Laboratory Cat#001976

Oligonucleotides TaqMan
TaqMan Hprt primer, Mm00446968_m1 Applied Biosystems
TaqMan IL33 primer Mm00505403_m1 Applied Biosystems
TaqMan ST2 primer Mm00516117_m1 Applied Biosystems
TaqMan Cebpα, Mm00514283_s1 Applied Biosystems
TaqMan Fabp4, Mm00445878_m1 Applied Biosystems
TaqMan Ppar, Mm01184322_m1 Applied Biosystems
TaqMan Alp, Mm00475834_m1 Applied Biosystems
TaqMan Sox9, Mm00448840_m1 Applied Biosystems
TaqMan Gapdh, Mm99999915_g1 Applied Biosystems
TaqMan Foxp3, Mm00475162_m1 Applied Biosystems
TaqMan Human Gapdh Hs02758991_m1 Applied Biosystems
TaqMan Human Il33, Hs04931857_m1 Applied Biosystems

Regent or Resource source identifier
Software and Algorithms FlowJo 9 software FlowJo, LLC https://www.flowjo.com, RRID:SCR_008520
GraphPad Prism 7 software GraphPad Software https://www.graphpad.com, RRID:SCR_002798
BD LSRFortessa BD Biosciences
BD FACSAria cell sorter BD Biosciences

Supplemental References

1. Gondo S, Okabe T, Tanaka T, Morinaga H, Nomura M, Takayanagi R, et al. Adipose tissue-derived and bone marrow-derived mesenchymal cells develop into different lineage of steroidogenic cells by forced expression of steroidogenic factor 1. Endocrinology. 2008;149(9):4717-25.
2. Kasagi S, Zhang P, Che L, Abbatiello B, Maruyama T, Nakatsukasa H, et al. In vivo-generated antigen-specific regulatory T cells treat autoimmunity without compromising antibacterial immune response. Science translational medicine. 2014;6(241):241ra78.